Molecular Therapy
Original Article

Long Noncoding RNA LINC00673 Is Activated by SP1 and Exerts Oncogenic Properties by Interacting with LSD1 and EZH2 in Gastric Cancer

Mingde Huang,[1,2,5] Jiakai Hou,[2,5] Yunfei Wang,[2,5] Min Xie,[3] Chenchen Wei,[4] Fengqi Nie,[4] Zhaoxia Wang,[4] and Ming Sun[2]

[1]Department of Medical Oncology, Huai'an First People's Hospital, Nanjing Medical University, Huai'an 223300, People's Republic of China; [2]Department of Bioinformatics and Computational Biology, University of Texas MD Anderson Cancer Center, Houston, TX 77030, USA; [3]Department of Biochemistry and Molecular Biology, Nanjing Medical University, Nanjing 210011, People's Republic of China; [4]Department of Oncology, Second Affiliated Hospital, Nanjing Medical University, Nanjing 210011, People's Republic of China

Long noncoding RNAs (lncRNAs) have emerged as important regulators in a variety of human diseases, including cancers. However, the biological function of these molecules and the mechanisms responsible for their alteration in gastric cancer (GC) are not fully understood. In this study, we found that lncRNA LINC00673 is significantly upregulated in gastric cancer. Knockdown of LINC00673 inhibited cell proliferation and invasion and induced cell apoptosis, whereas LINC00673 overexpression had the opposite effect. Online transcription factor binding site prediction analysis showed that there are SP1 binding sites in the LINC00673 promoter region. Next, luciferase reporter and chromatin immunoprecipitation (ChIP) assays provided evidence that SP1 could bind directly to the LINC00673 promoter region and activate its transcription. Moreover, mechanistic investigation showed that CADM4, KLF2, and LATS2 might be the underlying targets of LINC00673 in GC cells, and RNA immunoprecipitation, RNA pull-down, and ChIP assays showed that LINC00673 can interact with EZH2 and LSD1, thereby repressing KLF2 and LATS2 expression. Taken together, these findings show that SP1-activated LINC00673 exerts an oncogenic function that promotes GC development and progression, at least in part, by functioning as a scaffold for LSD1 and EZH2 and repressing KLF2 and LATS2 expression.

INTRODUCTION

Gastric cancer (GC) is the most common gastrointestinal malignancy and is the second leading cause of cancer-related deaths worldwide.[1,2] Although improvements in surgical techniques and chemotherapy have been made, the 5-year overall survival rate for patients with GC remains unsatisfactory.[3,4] In common with other cancers, GC tumorigenesis is a multistep process involving diverse genetic and epigenetic alterations and environmental factors.[5] However, the molecular mechanisms underlying GC carcinogenesis and progression are poorly understood. Recently, a number of studies have highlighted the critical roles played by long noncoding RNAs (lncRNAs) in the pathogenesis of several types of human cancer,[6,7] but little is known about the regulators that contribute to the alteration of these molecules and their involvement in GC.

Over the past decade, accumulating evidence from human genome sequencing, the Encyclopedia of DNA Elements (ENCODE) project, and GENCODE annotation[8,9] has revealed that less than 3% of the human genome constitutes protein coding genes, while the majority of the genome transcribes vast numbers of noncoding RNAs. lncRNAs are new regulatory RNA members with lengths greater than 200 nucleotides and no protein coding capacities.[10] Recent studies have revealed that lncRNAs participate in a wide range of biological processes, and alterations to them have been found to be involved in a variety of human diseases.[10–12] Furthermore, more and more cancer-associated lncRNAs have been characterized, and their functional roles and underlying mechanisms involved in tumorigenesis and cancer progression have been demonstrated.[13,14] In the case of GC, microarray and The Cancer Genome Atlas (TCGA) sequencing analyses have revealed that sets of lncRNAs are expressed differently in GC tumor tissues compared with normal tissues. Our previous studies have shown that overexpressed lncRNAs HOTAIR,[15,16] HOXA-AS2,[17] and ZFAS1[18] exhibit oncogenic functions in GC, while MEG3[19] and GAS5[20] act as tumor suppressors.

LINC00673 is an intergenic lncRNA located on 17q25.1, and a single nucleotide polymorphism (rs7214041) in this region was shown to be

Received 26 September 2016; accepted 18 January 2017;
http://dx.doi.org/10.1016/j.ymthe.2017.01.017.

[5]These authors contributed equally to this work.

Correspondence: Ming Sun, Department of Bioinformatics and Computational Biology, University of Texas MD Anderson Cancer Center, 1400 Pressler Street, Unit 1410, Houston, TX 77030, USA.
E-mail: msun7@mdanderson.org
Correspondence: Fengqi Nie, Department of Oncology, Second Affiliated Hospital, Nanjing Medical University, Nanjing 210011, People's Republic of China.
E-mail: 957714486@qq.com
Correspondence: Zhaoxia Wang, Department of Oncology, Second Affiliated Hospital, Nanjing Medical University, Nanjing 210011, People's Republic of China.
E-mail: zhaoxiawang88@hotmail.com

 © 2017 The American Society of Gene and Cell Therapy.

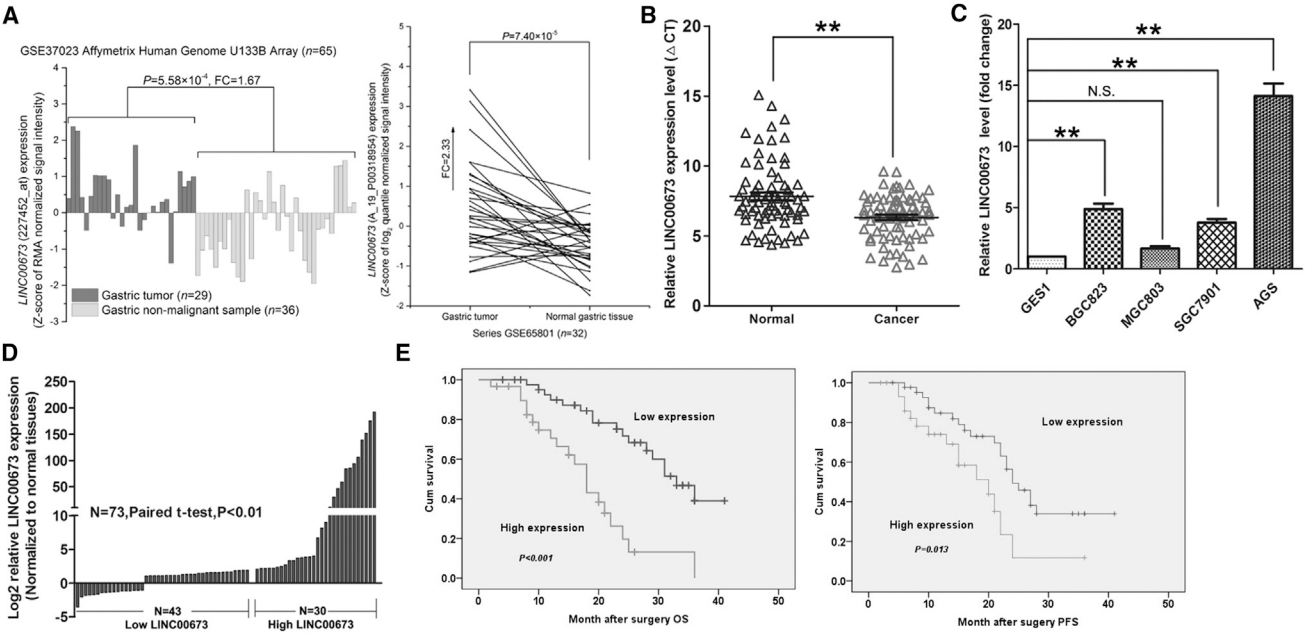

Figure 1. LINC00673 Is Highly Expressed in GC Tissues and Cells

(A) Data mining of LINC00673 for the GC tissue microarray gene profiling results (GSE37023 and GSE65801). (B) qRT-PCR analysis of LINC00673 expression in 73 paired GC tissues and their adjacent non-tumor tissues. LINC00673 levels were normalized to GAPDH expression. (C) qRT-PCR analysis of LINC00673 expression in cell lines BGC823, SGC7901, MGC803, AGS, and GSE1. LINC00673 levels were normalized to that of the GAPDH expression level. (D) Patients with GC were divided into two groups according to their LINC00673 expression profiles. A 2-fold change was used as the cutoff value. (E) Kaplan-Meier overall survival and disease-free survival analysis of the association between LINC00673 expression and GC patient survival ability. The mean values and SEs were calculated from triplicates of a representative experiment. **$p < 0.01$. N.S., not significant; OS, overall survival; PFS, progression-free survival.

significantly associated with pancreatic cancer risk.[21] Additionally, Zheng et al.[22] reported that LINC00673 could reinforce the interaction of PTPN11 with PRPF19 and promote PTPN11 degradation, resulting in diminished Src kinase-extracellular signal-regulated kinase (SRC-ERK) oncogenic signaling and enhanced activation of the STAT1-dependent antitumor response. A G > A change in exon 4 of LINC00673 (rs11655237) creates a binding site for miR-1231 and diminishes the effect of LINC00673, thereby conferring susceptibility to tumorigenesis. Conversely, Shi et al.[23] found that LINC00673 is significantly upregulated in non-small cell lung cancer (NSCLC) and exerts its oncogenic function by promoting cell growth. However, the expression pattern, function role, and underlying mechanism of LINC00673-related tumorigenesis in GC are unknown.

In this study, we investigated the expression profile, functional role, and underlying targets of LINC00673 in GC. We first determined that LINC00673 expression was significantly upregulated in GC tissues. Knockdown of LINC00673 suppressed cell growth and invasion, implying that LINC00673 might be an oncogenic lncRNA involved in GC development and progression. Furthermore, we found that transcription factor (TF) SP1 could activate LINC00673 transcription in GC cells. More importantly, LINC00673 can directly bind to LSD1 and EZH2, and may function as a scaffold for them, thereby repressing the underlying KLF2 target and LATS2 expression.

RESULTS

LINC00673 Is Upregulated in GC and Is Associated with Poor Prognosis

An analysis of GC tissue gene profiling data (GSE65801[24] and GSE37023[25]) showed that among 32 paired GC tumor and adjacent non-tumor tissues and 29 tumor and 36 adjacent non-tumor tissues, LINC00673 was expressed more highly in the tumor tissues (Figure 1A). To further validate this result, we investigated LINC00673 expression in a cohort of 73 paired GC tumors and adjacent non-tumor tissues using qRT-PCR. The results showed that LINC00673 expression was significantly higher in the tumor tissues (Figure 1B). Next, we examined LINC00673 levels in GC cell lines (BGC823, SGC7901, MGC803, and AGS) and GES1 using qRT-PCR. Compared with the GES1 cells, LINC00673 was present at higher levels in GC cells (Figure 1C). Collectively, these results show that LINC00673 is upregulated in GC tissues and cells. To further explore the relationship between LINC00673 expression and clinicopathology in patients with GC, patients were divided into two groups: the high LINC00673 expression group (n = 30, fold-change ≥ 2) and the low LINC00673 expression group (n = 40, fold-change ≤ 2) (Figure 1D). Statistical analysis revealed that higher LINC00673 levels were correlated with tumor size ($p = 0.019$), advanced pathological stage ($p = 0.024$), and lymph node metastasis ($p = 0.045$). However, LINC00673 expression was not associated with other factors including gender ($p = 0.474$) and age ($p = 0.352$) in GC (Table S1).

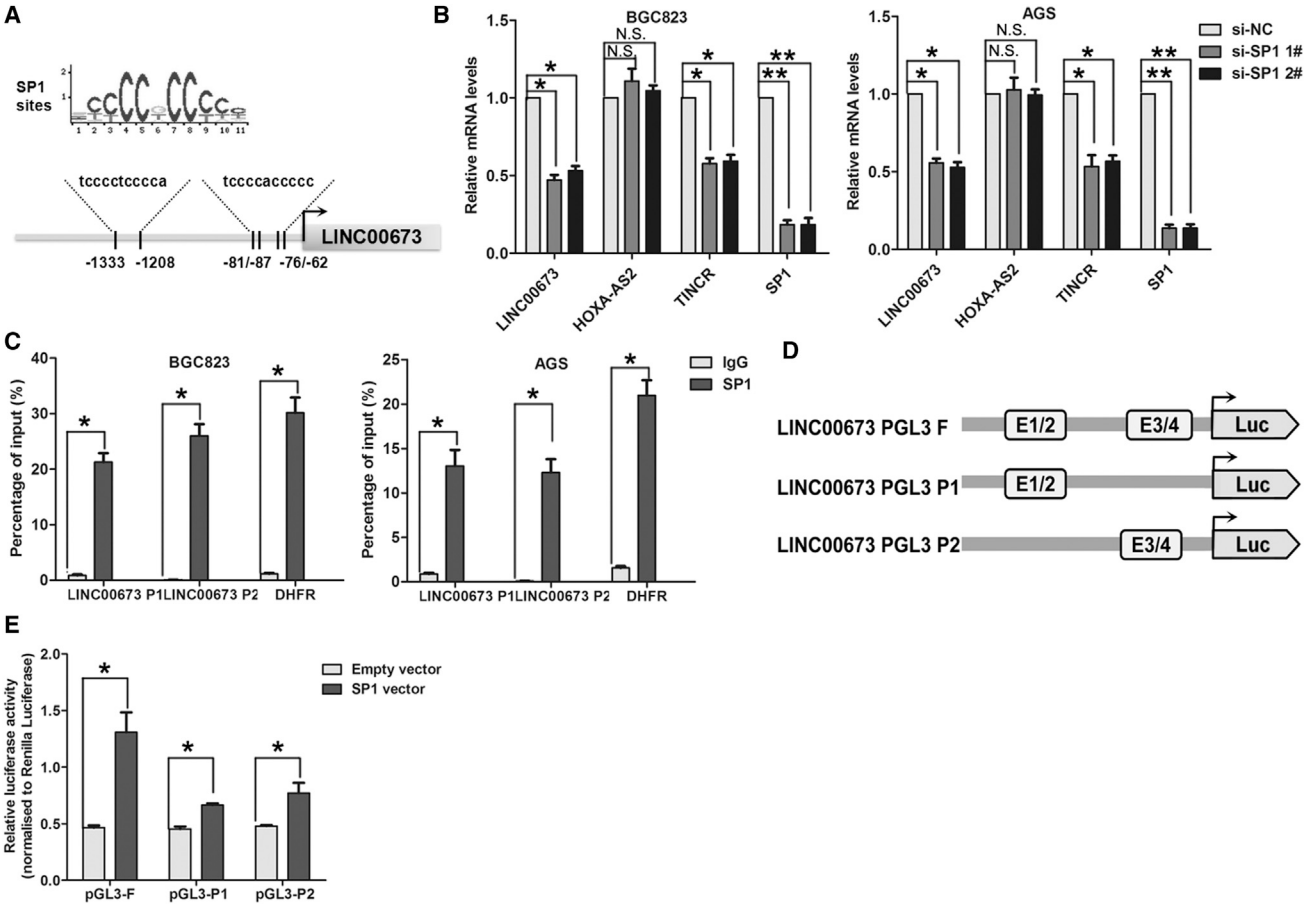

Figure 2. SP1 Activates LINC00673 Expression in GC Cells

(A) SP1 binding site prediction in the LINC00673 promoter region using JASPAR. (B) qRT-PCR analysis of LINC00673, TINCR, HOXA-AS2, and SP1 expression in BGC823 and AGS cells after transfection with SP1 siRNA or the negative control. (C) ChIP-qPCR analysis of SP1 occupancy in the LINC00673 promoter in BGC823 and AGS cells. DHFR was used as a positive control and IgG as a negative control. The mean values and SEs were calculated from triplicates of a representative experiment. (D) Construction of the luciferase reporter vector pGL3F (containing all SP1 binding sites), pGL3P1 (containing -1,333 and -1,208 binding sites), and pGL3P2 (containing -81 of 87 and -62 of 76 binding sites). (E) Luciferase assays of the cells indicated that were transfected with pGL3F, pGL3P1, or pGL3P2 vectors, the SP1 vector, or an empty vector. The mean values and SEs were calculated from triplicates of a representative experiment. *$p < 0.05$, **$p < 0.01$.

Next, we used a Kaplan-Meier survival analysis to examine the correlation between LINC00673 expression and the prognosis of patients with GC. The results showed that patients with higher LINC00673 levels had shorter overall survival and progression-free survival times than those with lower LINC00673 levels (Figure 1E). These findings suggest that upregulated LINC00673 may have an oncogenic function in GC. Moreover, univariate and multivariate Cox regression analyses showed that LINC0067 expression ($p = 0.024$) and lymph node metastasis ($p = 0.047$) were independent prognostic factors for patients with GC (Table S2).

SP1 Activates LINC00673 Transcription

Although a lot of lncRNA dysregulation has been reported in cancers, the regulators involved in misregulation of these molecules are not properly understood. Using the JASPAR online database, we selected transcription factor SP1, which is predicted to be bound to the LINC00673 promoter region with high scores, for analysis. The predicted binding sites of SP1 in the LINC00673 promoter sequence are illustrated in Figure 2A. We then transfected BGC823 and AGS cells with SP1 small interfering RNAs (siRNAs), and the qRT-PCR results showed that LINC00673 expression as well as TINCR (a known SP1 target lncRNA in GC) were downregulated after knockdown of SP1, while HOX-AS2 (without the SP1 binding site in the promoter) expression experienced no change in the SP1 knockdown cells (Figure 2B). Moreover, we designed two primers that covered the SP1 binding sites and performed chromatin immunoprecipitation (ChIP) assays to validate whether SP1 could bind to these sites. The ChIP results showed that SP1 could bind to both sites, and DHFR, a known SP1 target, was used as a positive control (Figure 2C). Next, we constructed the following three luciferase reporter plasmids: pGL3-F (containing all SP1 binding sites), pGL3-P1 (containing −1,333 and −1,208 sites) and pGL3-P2 (containing −81 and −76

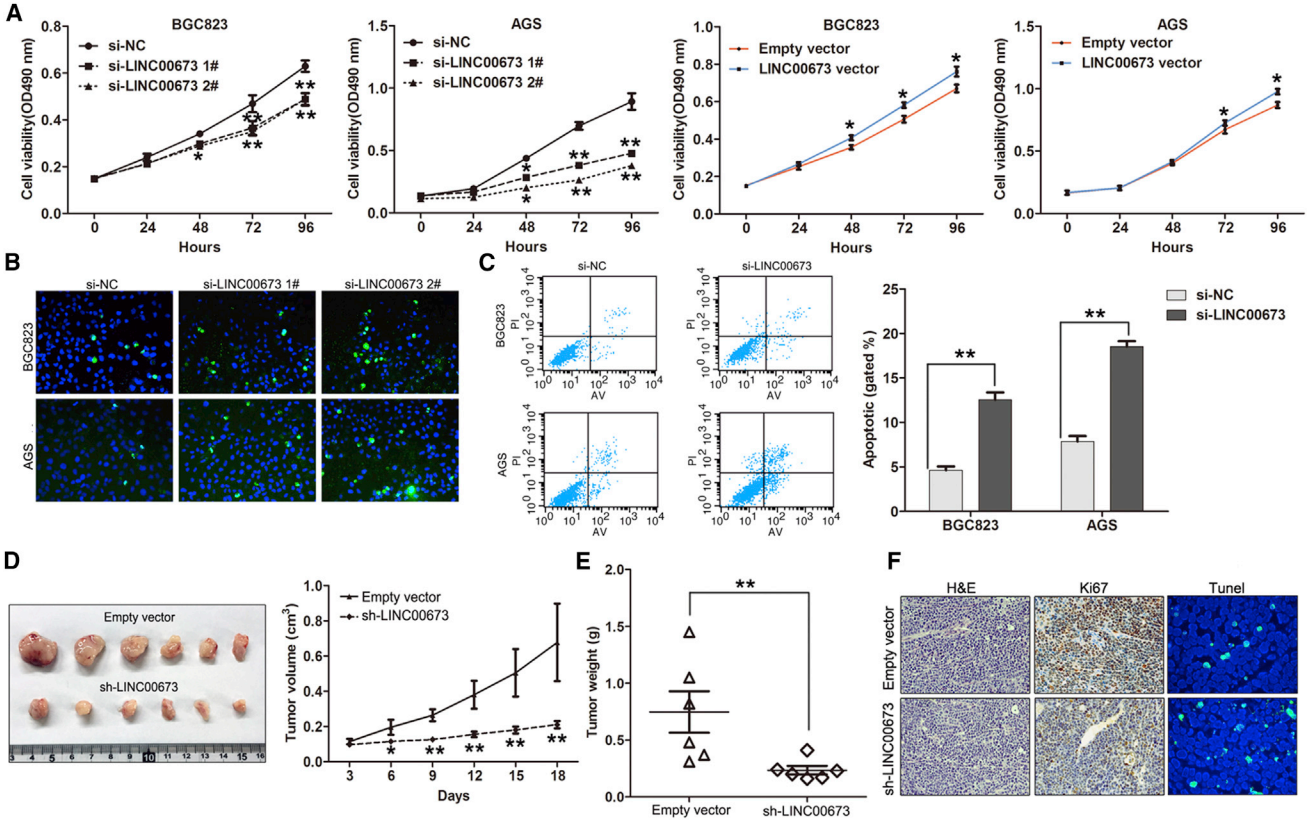

Figure 3. LINC00673 Knockdown Inhibits GC Cell Growth and Induces Apoptosis In Vitro and In Vivo

(A) Growth curves for BGC823 and AGS cells after transfection with LINC00673 siRNA or the negative control were determined by MTT assays. (B) BGC823 and AGS cell apoptosis after transfection with LINC00673 siRNA or the negative control was evaluated by TUNEL staining assays. Dead cells were labeled with TUNEL (green); nuclear fractions were labeled with DAPI (blue). (C) BGC823 and AGS cell apoptosis after transfection with LINC00673 siRNA or the negative control was evaluated by flow cytometry by measuring the percentage of Annexin V-stained cells. (D) AGS cells stably expressing LINC00673 shRNA or the negative control were used for in vivo tumorigenesis. Tumor growth curves after subcutaneous injection of AGS cells containing a stable knockdown of LINC00673 or the negative control are shown. The tumor volumes were measured every 3 days after inoculation. (E) Tumor weights are represented. (F) Ki67 protein levels and apoptotic cells in tumor tissues from sh-LINC00673 or negative control transfected AGS cells were determined by immunohistochemistry and TUNEL staining. The mean values and SEs were calculated from triplicates of a representative experiment. *$p < 0.05$, **$p < 0.01$.

sites) (Figure 2D). Dual luciferase reporter assays showed that SP1 could bind to both the E1/2 and E3/4 elements and activate luciferase, and the luciferase reporter containing both E1/2 and E3/4 had higher luciferase activity than that containing only E1/2 or E3/4 (Figure 2E). These findings indicate that some TFs can contribute to human cancer development and progression not only through affecting protein coding genes expression but also via regulating noncoding genes such as lncRNAs transcription.

Knockdown of LINC00673 Inhibits Cell Growth and Induces Apoptosis In Vitro and In Vivo

To determine the biological functions of LINC00673 in GC cells, LINC00673 expression was knocked down in BGC823 and AGS cells by transfection with siRNA or short hairpin RNA (shRNA) vector and was overexpressed by transfection with an LINC00673 overexpression vector (Figures S1A and S1B). To assess the role of LINC00673 in the GC cell phenotype, we performed loss-of-function and gain-of-function assays. The MTT assays showed that the growth of BGC823 and AGS cells transfected with si-LINC00673 was inhibited compared with the control cells, while LINC00673 overexpression promoted BGC823 and AGS cell proliferation (Figure 3A). EdU staining assays also showed that decreased LINC00673 expression inhibited BGC823 and AGS cell proliferation (Figure S1C). Moreover, colony formation analysis showed that LINC00673 knockdown significantly impaired the colony formation capacity of the GC cells, while LINC00673 overexpression increased BGC823 and AGS cell colony formation (Figure S2). Because the above results indicate that LINC00673 exerts an oncogenic effect in GC cells, we then investigated whether LINC00673 is involved in regulating cell apoptosis using flow cytometry and terminal deoxynucleotidyl transferase dUTP nick-end labeling (TUNEL) staining analyses. Compared with the control cells, knockdown of LINC00673 significantly increased the GC cell apoptotic rate (Figures 3B and 3C).

We next injected the LINC00673 stable knockdown of AGS cells or control cells into nude mice to determine whether LINC00673 could influence GC cell tumorigenesis in vivo. The results showed that tumors grown from LINC00673 stable knockdown cells were smaller than tumors grown from the control cells (Figure 3D). The tumor weight of the sh-LINC00673 group was also significantly lower than that of the control group (Figure 3E). qRT-PCR assays determined that the LINC00673 expression levels were downregulated in tumor tissues collected from the sh-LINC00673 group compared with the controls (Figure S3A). Finally, immunohistochemistry analysis confirmed that the tumors formed from AGS/sh-LINC00673 cells displayed lower Ki-67 staining and higher TUNEL staining signals than those formed from the control cells (Figure 3F).

Effect of LINC00673 on Cell Migration, Invasion, and Metastasis in GC

To evaluate whether LINC00673 contributes to the progression of GC, we examined the effect of LINC00673 on the migration and invasive behavior of BGC823 and AGS cells. Using a transwell assay, we found that the migration and invasive ability of the GC cells was dramatically impaired following siRNA-mediated downregulation of LINC00673 (Figures 4A–4C). Conversely, LINC00673 overexpression increased the migration and invasive ability of the GC cells (Figures 4D and 4E). Taken together, these data suggest that LINC00673 plays critical roles in GC progression.

To validate the in vitro results, BGC823 cells stably transfected with empty vector or sh-LINC00673 vector were injected into nude mice. As shown in Figure 4F, downregulation of LINC00673 resulted in a reduction in metastatic nodules on the mice lungs when compared with those in the control group. Furthermore, this difference was confirmed following the H&E staining of lung sections (Figure 4G). These results indicate that LINC00673 is also involved in human GC progression through affecting cancer cell invasion and metastasis.

CADM4, LATS2, and KLF2 Are Key Downstream Targets of LINC00673

To investigate the potential genes involved in LINC00673 function in GC cells, we used an RNA-sequencing analysis. As shown in Figure 5A, the expression levels of many genes involved in cell proliferation and cell-cell junction regulation were differentially expressed in the LINC00673 knockdown cells compared with the control. Next, several genes that may contribute to GC development and progression were selected and their regulation was confirmed by qRT-PCR assays (Figure 5B). Additionally, a correlation analysis showed that LINC00673 expression also negatively correlates with tumor suppressor KLF2 and LATS2 expression in GC tissues (Figure 5C). Importantly, LATS2 and KLF2 expression increased in GC cells after LINC00673 knockdown (Figure 5D). Therefore, we selected CADM4, KLF2, and LATS2, which have been found to be involved in cancer cell proliferation, apoptosis, and invasion, respectively, as potential LINC00673 targets. Thereafter, western blot analysis showed that LINC00673 knockdown significantly upregulated CADM4, LATS2, and KLF2 protein levels in GC cells (Figures 5E and 5F).

LINC00673 Represses LATS2 and KLF2 Expression by Interacting with LSD1 and EZH2

Generally, lncRNAs regulate their target genes by interacting with RNA binding proteins or acting as endogenous competing RNAs for specific microRNAs (miRNAs). To investigate the molecular mechanism underlying LINC00673-associated regulation of its targets in GC cells, we first analyzed the distribution of LINC00673 in GC cells using fluorescence in situ hybridization (FISH) and subcellular fractionation analyses. The results showed that LINC00673 is distributed in both the cytoplasm and nucleus, but the ratio of LINC00673 in the nucleus is higher (Figures 6A and 6B). Then, we predicted the interaction probabilities between LINC00673 and RNA binding proteins via RNA-protein interaction prediction (http://pridb.gdcb.iastate.edu/RPISeq/), and we found that LINC00673 potentially binds EZH2, LSD1, SUZ12, AGO2, and STAU1 (with RF or support vector machine [SVM] scores >0.5, Figure S3B). We next performed radioimmunoprecipitation assays and confirmed that LINC00673 binds directly to EZH2, LSD1, DNMT1, and STAU1 in GC cells, while U1 binding with SNRNP70 and HOTAIR binding with EZH2 and LSD1 were used as positive controls (Figures 6C and S3C and S3D). Moreover, RNA pull-down assays further confirmed that LINC00673 indeed binds with EZH2, LSD1, and STAU1 in GC cells (Figure 6D). These data suggest that LINC00673 can epigenetically repress underlying target expression at the transcriptional level.

To determine whether proteins interacting with LINC00673 are involved in regulating CADM4, LATS2, and KLF2, we treated BGC823 and AGS cells with EZH2 and LSD1 siRNAs. The results showed that knockdown of EZH2 and LSD1 both increased LATS2 and KLF2 expression, while knockdown of EZH2 and LSD1 had no effect on CADM4 expression in BGC823 and AGS cells (Figures 6E and 6F). We next performed chromatin immunoprecipitation assays and found that EZH2 and LSD1 could directly bind to the promoter regions of LATS2 and KLF2 and induce H3K27 trimethylation or H3K4 demethylation (Figures 6G and S4A). Importantly, LINC00673 knockdown decreased their binding ability and induced modification (Figure 6H). The above results indicate that LINC00673 regulates its underlying targets in GC cells mainly through recruiting RNA binding proteins such as EZH2 and LSD1 to the promoter regions of targets and inducing histone modification.

LINC00673 Oncogenic Function Is Partly Dependent on Repressing LATS2 and KLF2 Expression

To further determine whether LATS2 and KLF2 function as tumor suppressors in GC, we first detected their expression levels in normal and tumor tissues. The results showed that LATS2 and KLF2 expression are both downregulated in tumor tissues (Figure S4B). Then, we performed gain-of-function assays by transfection with LATS2 and KLF2 vectors in AGS and BGC823 cells. Using an MTT assay, we

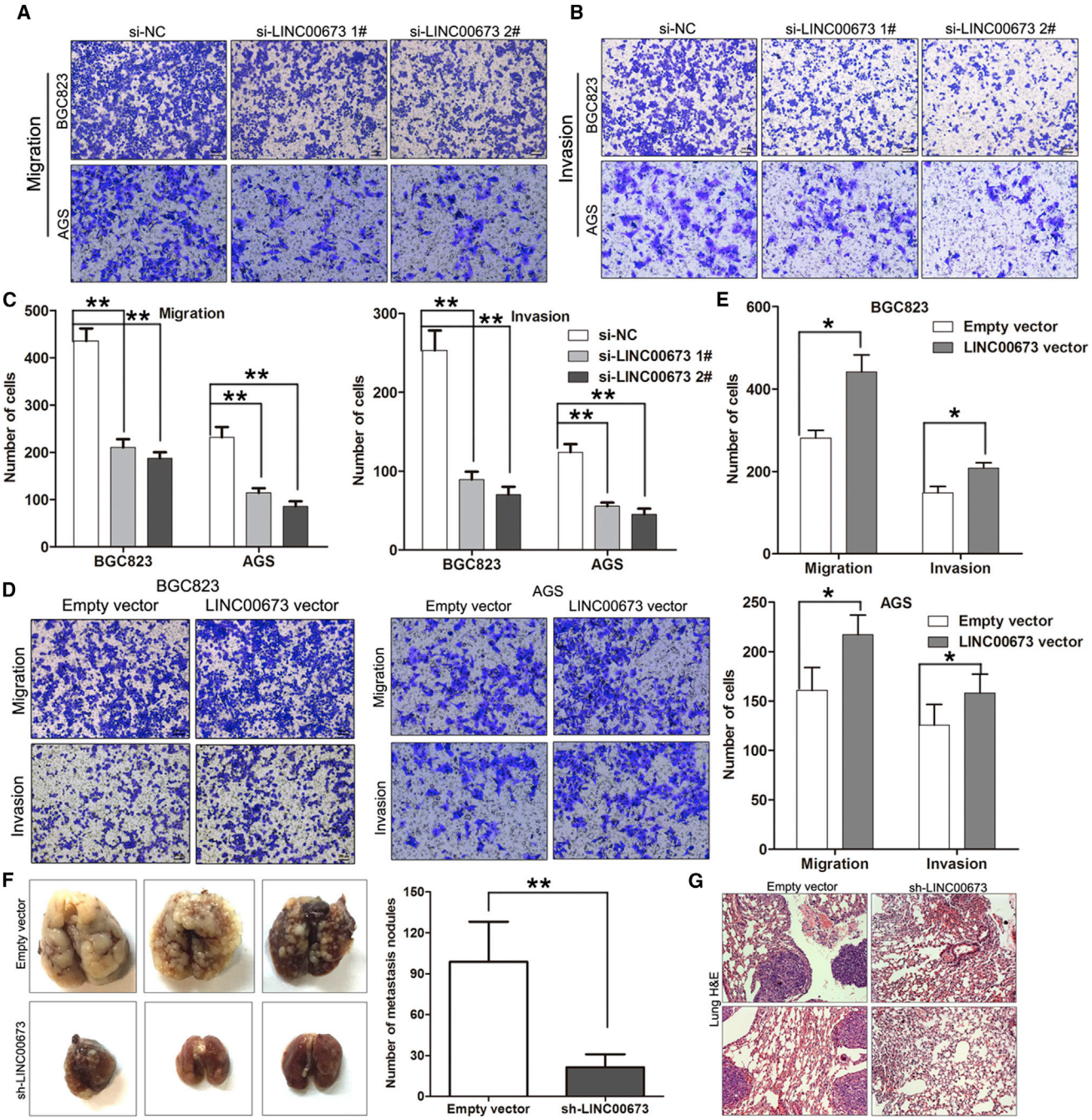

Figure 4. LINC00673 Promotes Cell Migration and Invasion In Vitro

(A–C) The migration and invasive ability after knockdown of LINC00673 in BGC823 and AGS cells was assessed using transwell assays. (D and E) The migration and invasive ability after upregulation of LINC00673 in BGC823 and AGS cells was assessed using transwell assays. The mean values and SEs were calculated from triplicates of a representative experiment. (F) An experimental metastasis animal model was performed by injecting LINC00673 stable knockdown BGC823 cells into the tail vein of nude mice. (Left) Lungs from each group are shown. (Right) The number of tumor nodules on lung surfaces from two groups are shown. (G) Visualization of the H&E-stained lung sections. The mean values and SEs were calculated from triplicates of a representative experiment. *$p < 0.05$, **$p < 0.01$.

found that overexpression of LATS2 and KLF2 significantly inhibited AGS and BGC823 cell proliferation (Figures 7A–7C). Moreover, the results of the transwell analysis showed that upregulated LATS2 and KLF2 inhibited AGS and BGC823 cell invasive abilities (Figure 7D). To determine whether LATS2 and KLF2 are involved in the LINC00673-induced increase in GC cell proliferation and

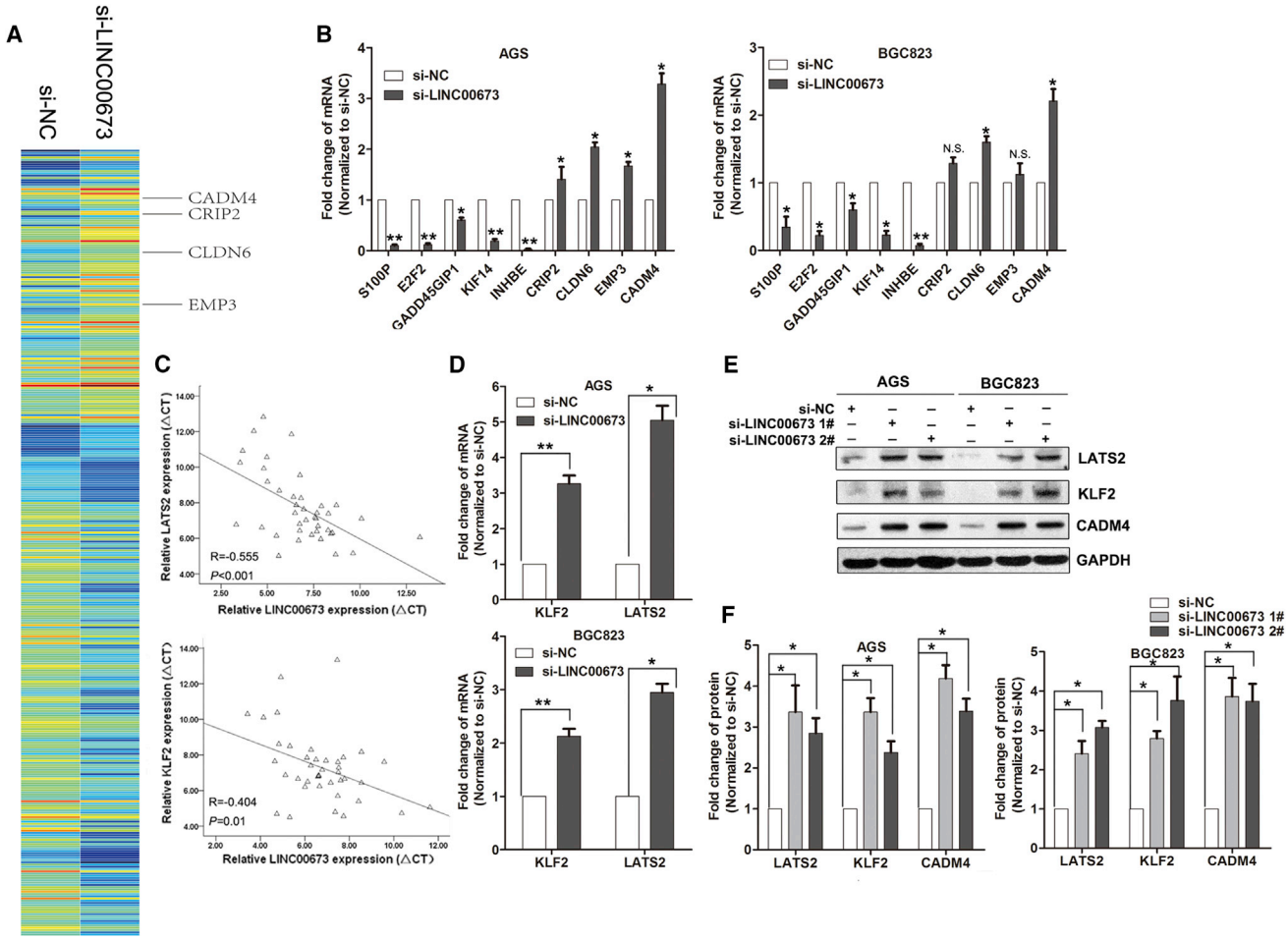

Figure 5. CADM4, KLF2, and LATS2 Are Underlying Targets of LINC00673

(A) Hierarchically clustered heatmap of upregulated and downregulated genes in AGS cells after transfection with LINC00673 or NC siRNAs. (B) qRT-PCR analysis of S100, E2F2, GADD45GIP1, KIF14, INHBE, CRIP2, CLDN6, EMP3, and CADM4 expression in AGS and BGC823 cells after transfection with LINC00673 or NC siRNA. (C) Association analysis of the relationship between LINC00673 and KLF2 expression levels, and LINC00673 and LATS2 expression levels, in 20 paired GC tissues. (D) qRT-PCR analysis of LATS2 and KLF2 expression in AGS and BGC823 cells after transfection with LINC00673 or NC siRNA. (E and F) CADM4, KLF2, and LATS2 protein levels were detected in AGS and BGC823 cells after transfection with LINC00673 siRNAs or negative control by western blotting. The mean values and SEs were calculated from triplicates of a representative experiment. *$p < 0.05$, **$p < 0.01$.

invasion, we performed rescue experiments. AGS cells were co-transfected with LINC00673, LATS2, or KLF2 siRNAs (Figure 7E). MTT and transwell assays showed that knockdown of LATS2 and KLF2 partly rescued the LINC00673 downregulation-induced cell growth arrest and invasion decrease in AGS cells (Figures 7F and 7G).

Collectively, these results demonstrate that LINC00673 overexpression plays an important role in human gastric cancer development and progression through promotion of GC cell proliferation and invasion, which partly depends on regulation of LATS2 and KLF2 expression via interacting with EZH2 and LSD1. Additionally, LINC00673 overexpression in human GC cells is partly due to transcription factor SP1 binding to its promoter region and promoting the transcription (Figure 8).

DISCUSSION

lncRNAs have emerged as critical players in tumorigenesis and cancer progression processes; however, the potential function(s) and mechanistic details for most lncRNAs in human GC still remain unclear. Here, we found that LINC00673 is significantly upregulated in GC tissues and cells. Increased LINC00673 expression is associated with a poor prognosis in patients with GC and shorter overall and progression-free survival times. Using loss-of-function and gain-of-function assays, we showed that the lncRNA, LINC00673, plays a critical role in GC cell proliferation and invasion. Knockdown of LINC00673 significantly decreased GC cell growth, induced apoptosis, and inhibited migration and invasion, whereas overexpression of LINC00673 had the opposite effects. These findings suggest that LINC00673 functions as an oncogene

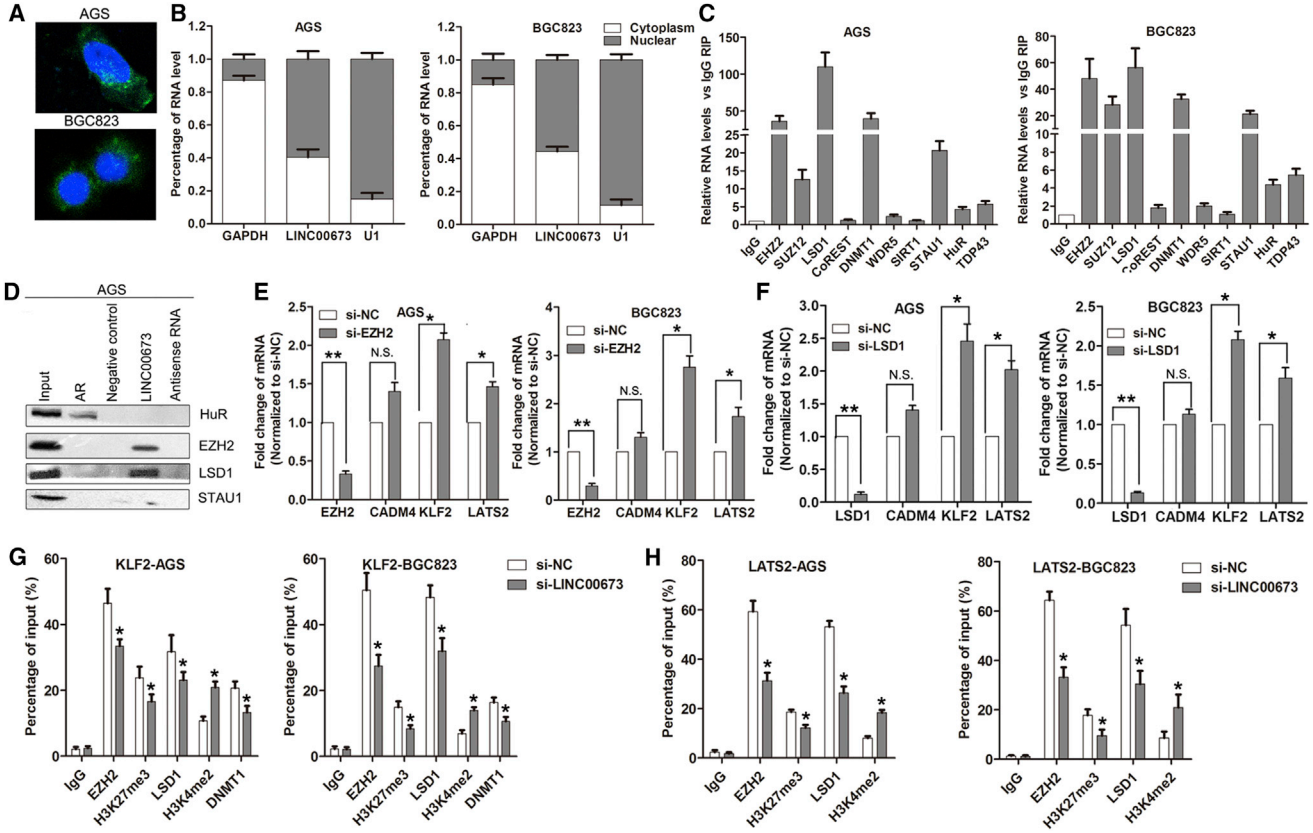

Figure 6. LINC00673 Suppresses LATS2 and KLF2 Transcription by Binding to EZH2 and LSD1

(A) FISH analysis of the location of LINC00673 (green) in the cytoplasm and nuclear fractions (blue) of BGC823 and SGC7901 cells. (B) qRT-PCR detection of the percentage of LINC00672, U1, and GAPDH in the cytoplasm and nuclear fractions of BGC823 and AGS cells. GAPDH and U1 were used as cytoplasmic and nuclear localization markers, respectively. (C) LINC00673 RNA levels in immunoprecipitates were determined by qRT-PCR. LINC00673 RNA expression levels are presented as fold enrichment values relative to IgG immunoprecipitates. (D) HuR, EZH2, LSD1, and STAU1 protein levels in immunoprecipitates with LINC00673 RNA were evaluated by western blots. Androgen receptor (AR) RNA was used as a positive control for HuR protein. The expression levels of HuR, EZH2 and LSD1 proteins are shown. (E) qRT-PCR analysis of CAMD4, LATS2, KLF2, and EZH2 expression in BGC823 and AGS cells after transfection with EZH2 or NC siRNA. (F) qRT-PCR analysis of CAMD4, LATS2, KLF2, and LSD1 expression in BGC823 and AGS cells after transfection with LSD1 or NC siRNA. (G) ChIP-qPCR analysis of EZH2, H3K27me3, LSD1, and H3K4me2 occupancy in the KLF2 promoter in BGC823 and AGS cells after transfection with LINC00673 or NC siRNA, with IgG used as a negative control. (H) ChIP-qPCR analysis of EZH2, H3K27me3, LSD1, and H3K4me2 occupancy in the LATS2 promoter in BGC823 and AGS cells after transfection with LINC00673 or NC siRNA, with IgG used as a negative control. The mean values and SEs were calculated from triplicates of a representative experiment. *$p < 0.05$, **$p < 0.01$.

in GC, and its overexpression contributes to GC tumorigenesis and progression.

A recent genome-wide association study analyzing 7,956 newly genotyped PanC4 individuals revealed that LINC00673 loci (17q25, 1rs7214041) are significantly associated with pancreatic cancer risk.[21] In contrast with our observations, Zheng et al.[22] found that LINC00673 acts as a potential tumor suppressor by reinforcing the interaction of PTPN11 with PRPF1 in pancreatic cancer (PDC), which suggests that LINC00673 may exert an oncogene or tumor suppressor function depending on the tissue-specific expression pattern and circumstances. However, the regulators responsible for lncRNA deregulation in different cancers are still not thoroughly elucidated. Recently, accumulating evidence has shown that lncRNA expression can be regulated in a manner similar to protein coding genes. For instance, our previous studies indicate that epigenetic regulation modulates the expression of lncRNA SPRY4-IT1 and MEG3 through promoter-associated histone and DNA methylation in NSCLC,[26,27] and transcription factor E2F1 activates ANRIL expression in GC.[28] In the current study, we found that LINC00673 expression could be activated by transcription factor SP1 through binding to its promoter region. These data indicate that the unique lncRNA expression pattern found in different cancers may be related to the regulation of different regulators.

There is evidence to show that lncRNAs regulate target expression through distinct mechanisms in different cancer cells. Applying RNA immunoprecipitation (RIP) and RNA pull-down analysis, we

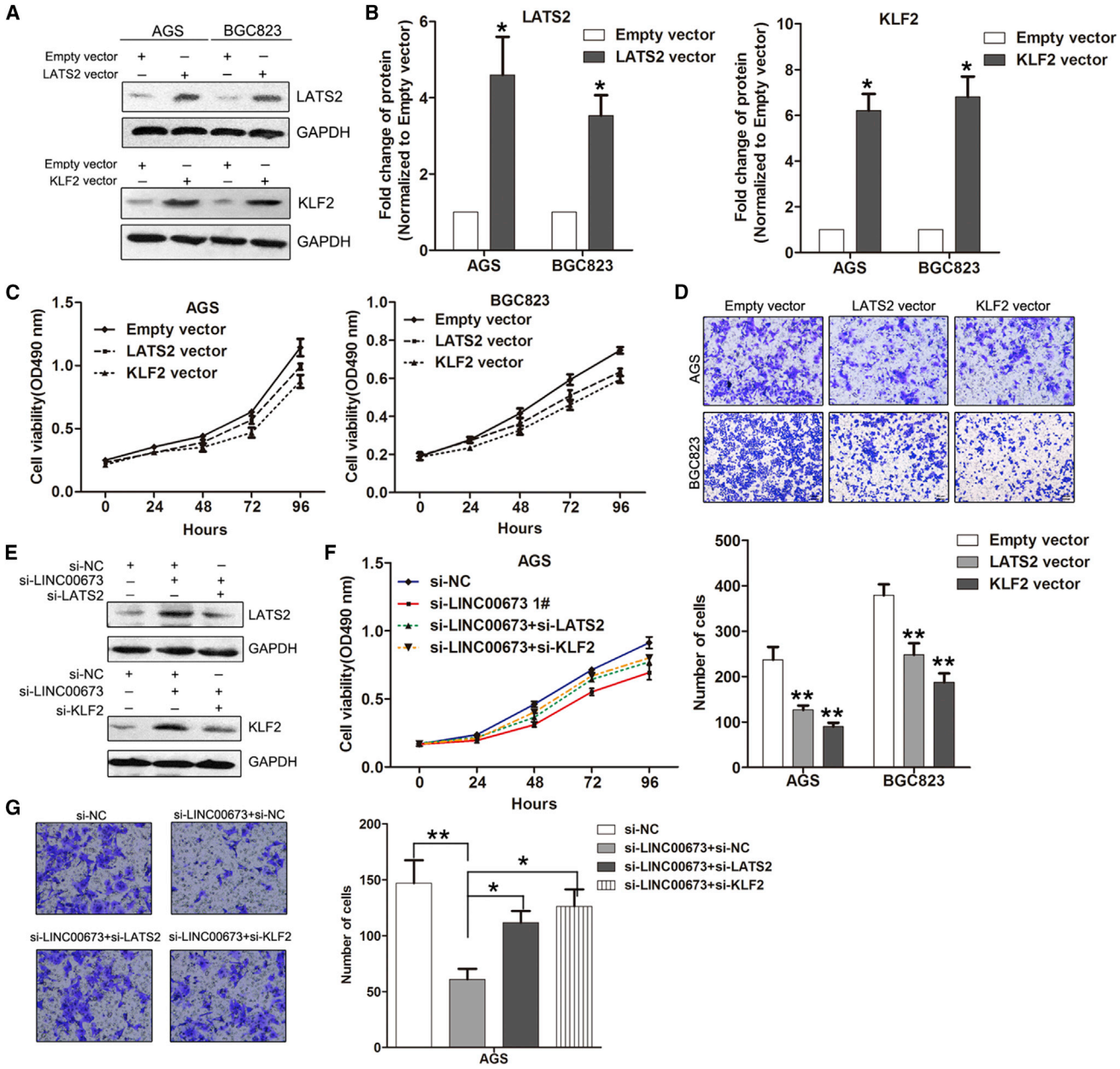

Figure 7. LINC00673 Exhibits Oncogenic Properties Partly Dependent on LATS2 and KLF2 Silencing

(A and B) Western blot detection of LATS2 and KLF2 protein levels in BGC823 and AGS cells after transfection with LATS2 or KLF2 vectors. (C) AGS and BGC823 cell growth curves after transfection with LATS2, KLF, or empty vector were determined by MTT assays. Values represent the mean ± SE of three independent experiments. (D) The effect of LATS2 and KLF2 overexpression on the invasion of AGS and BGC823 cells was assessed using transwell assays. (E) Western blot detection of the LATS2 and KLF2 protein levels in AGS cells after co-transfection with LINC00673, LATS2, KLF2, or NC siRNAs. (F) Growth curves for AGS cells after co-transfection with LINC00673, LATS2, KLF2, or NC siRNAs were determined by MTT assays. Values represent the mean ± SE of three independent experiments. (G) The invasive abilities of AGS cells after co-transfection with LINC00673, LATS2, KLF2, or NC siRNAs were determined by transwell assays. The mean values and SEs were calculated from triplicates of a representative experiment. *$p < 0.05$, **$p < 0.01$.

showed that LINC00673 could bind directly to several RNA binding proteins, including EZH2, SUZ12, LSD1, and STAU1. Further high-throughput RNA sequencing and correlation analysis showed that CADM4, LATS2, and KLF2 may be novel targets of LINC00673 in GC cells. However, knockdown of EZH2 or LSD1 had no effect on the CADM4 expression level but increased LATS2 and KLF2 expression levels in GC cells, suggesting that LINC00673 may regulate CADM4 through other mechanisms such as RNA decay, as

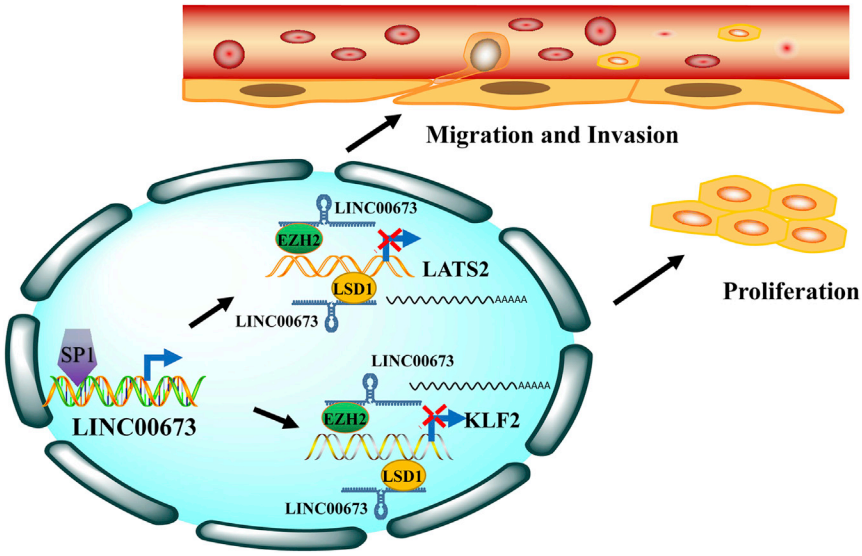

Figure 8. Summary of the Regulation and Mechanism of LINC00673 in GC

LINC00673 can also interact with STAU1. Importantly, ChIP assays determined that LINC00673 could simultaneously recruit EZH2 and LSD1 to LATS2 and KLF2 promoter regions, respectively, and repress their transcription. KLF2 is a Kruppel-like factor (KLF) family member, and these members contain Cys2/His2 zinc-finger domains and act as transcriptional repressors or activators to regulate multiple gene transcription.[29,30] Several studies have shown that KLF2 expression is diminished in multiple cancers and exhibits tumor-suppressor features for its inhibitory effect on cell proliferation and induction of cell apoptosis.[31,32] The tumor suppressor LATS2, which encodes a serine/threonine protein kinase, is a core member of the Hippo pathway that controls progenitor cell proliferation and survival, as well as tissue growth through silencing the transcriptional coactivators, YAP and TAZ.[33] Accumulating evidence shows that LATS2 expression is downregulated in many cancers.[34,35] For example, LATS2 expression is frequently downregulated in breast cancer, which results in shifting p53's conformation and transcriptional output and endowing p53 with the ability to promote cell migration.[36] Herein, we also found that KLF2 and LATS2 are downregulated in GC, and their overexpression impaired cell growth and invasion. Interestingly, rescue experiments determined that LINC00673's oncogenic function partly depends on repressing KLF2 and LATS2 expression.

In summary, our study showed for the first time that lncRNA LINC0673 expression is upregulated in GC tissues, is associated with poor prognosis, and may be a negative prognostic factor for patients with GC. Its effects on GC cell proliferation and invasion indicate that it exhibits oncogenic properties in GC tumorigenesis and progression. Transcription factor SP1 binds directly to the LINC00673 promoter and activates its transcription, while LINC00673 exerts its oncogenic effects partially through epigenetic silencing of LATS2 and KLF2 expression via acting as a scaffold for EZH2 and LSD1. Our findings further the understanding of GC pathogenesis and facilitate the development of lncRNA-directed diagnostics and therapeutics against this disease.

MATERIALS AND METHODS

Microarray Data Analysis

Three human microarray datasets, including GSE65801 and GSE37023, were obtained from the public GEO database (http://www.ncbi.nlm.nih.gov/geo) and normalized using the robust multichip average. After the probe sequences were downloaded from GEO or microarray manufacturers, blast+2.2.30 was used to re-annotate the probes according to the GENCODE Release 21 sequence database for lncRNA. For RNA sequencing, total RNA from AGS cells was used for sequencing on a HiSeq 2000 system (Illumina). Cuffdiff was used to compare the log ratio of FPKM in two conditions [i.e., log(FPKMa/FPKMb)] in the following test statistic, which is approximately normally distributed. A corresponding p value and an FDR-adjusted p value were also calculated.

Clinical Specimens and Cell Lines

GC specimens and their corresponding adjacent noncancerous tissues were obtained from the Second Affiliated Hospital of Nanjing Medical University between 2010 and 2011 with informed consent. The patients were diagnosed with GC based on histopathological evaluation, and no local or systemic treatment was conducted before surgery. The protocols used in the study were approved by the Research Ethics Committee of Nanjing Medical University. BGC823, SGC7901, MGC803, and AGS cell lines and a normal gastric epithelium cell line (GES-1) were purchased from the Shanghai Cell Bank of the Chinese Academy of Sciences. BGC823 and MGC803 cells were cultured in RPMI 1640 (Invitrogen); GES1, SGC7901, and AGS were cultured in DMEM with 10% fetal bovine serum (Invitrogen). All cell lines were characterized by DNA fingerprinting using short tandem repeat markers from the Shanghai Cell Bank.

RNA Extraction and qRT-PCR Assays

Total RNA from specimens and cells was isolated with TRIzol reagent (Invitrogen) according to the manufacturer's instructions. RNA (1 μg) was reverse transcribed in a final volume of 20 μL under the standard conditions used for the PrimeScript RT reagent kit (Takara). SYBR Premix Ex Taq (Takara) was used for the real-time qPCR assays, which were performed on an Applied Biosystems 7500 Real-Time PCR System. The primers sequences used are shown in Table S1. qRT-PCR results were analyzed and expressed relative to the threshold cycle (CT) values and then converted to fold changes.

Cell Transfection

Human LINC00673 cDNA and short hairpin RNA directed against LINC00673 were inserted into the vector. Plasmid vectors (pCDNA-LINC00673, sh-LINC00673, and empty vectors) for transfection were prepared using DNA Miniprep or Midiprep kits (QIAGEN) and then transfected into cells. si-LINC00673, si-SP1, si-EZH2, si-LSD1, or negative control siRNAs were used to knock-down expression, and all siRNA and shRNA sequences are shown in Table S1. GC cells were grown in six-well plates and transfected by Lipofectamine 2000 (Invitrogen) according to the manufacturer's instructions. At 48 hr post-transfection, cells were harvested for qRT-PCR or western blot analyses.

Cell Proliferation Assays

Cell proliferation ability was examined using Cell Proliferation Reagent Kit I (MTT; Roche Applied Science) and an EdU assay kit (Life Technologies). Colony formation assays were performed to monitor the cloning capabilities of the GC cells.

Cell Apoptosis Assays

BGC-823 and AGS cells transfected with si-LINC00673 or small interfering RNA negative control (si-NC) were harvested 48 hr after transfection by trypsinization. After double staining with fluorescein isothiocyanate (FITC)-Annexin V and propidium iodide, the cells were analyzed by flow cytometry (FACScan; BD Biosciences) equipped with CellQuest software (BD Biosciences).

In Vivo Tumor Formation Assay

Four-week-old female athymic BALB/c nude mice were maintained under specific pathogen-free conditions and manipulated according to the protocols approved by the Shanghai Medical Experimental Animal Care Commission. sh-LINC00673 or empty vector stably transfected AGS cells were harvested. For the tumor formation assay, 10^7 cells were injected subcutaneously into one side of each mouse. Tumor growth was examined every 3 days, and tumor volumes were calculated using the following equation: $V = 0.5 \times D \times d2$ (V, volume; D, longitudinal diameter; and d, latitudinal diameter). This study was carried out in strict accordance with the recommendations in the NIH Guide for the Care and Use of Laboratory Animals. The protocol was approved by the Committee on the Ethics of Animal Experiments of Nanjing Medical University.

RIP

RIP was used to investigate whether LINC00673 could interact or bind to potential binding proteins (e.g., EZH2, SUZ12, LSD1, and STAU1, among others) in GC cells. We used an EZMagna RIP kit (Millipore) to investigate this, following the manufacturer's protocol. BGC-823 and AGS cells were lysed in complete RIP lysis buffer, and the extract was incubated with magnetic beads conjugated with antibodies that recognized EZH2, SUZ12, and LSD1 (and others) or control immunoglobulin G (IgG) (Millipore) for 6 hr at 4°C. Next, the beads were washed and incubated with Proteinase K to remove the proteins. Finally, purified RNA was subjected to qRT-PCR analysis to show the presence of LINC00673 using specific primers.

RNA Pull-Down Assays

LINC00673 transcripts were transcribed using T7 RNA polymerase (Ambion Life) in vitro, then by using the RNeasy Plus Mini Kit (QIAGEN) and treated with DNase I (QIAGEN). Purified RNAs were biotin-labeled using Biotin RNA Labeling Mix (Ambion Life). The positive control, negative control, and biotinylated RNAs were mixed and incubated with AGS cell lysates. Then, magnetic beads were added to each binding reaction, and the mixtures were incubated at room temperature. Finally, the beads were washed, and the eluted proteins were detected by western blot analysis.

Luciferase Reporter Assays

The SP1 binding motif in the promoter region of LINC00673 was identified by JASPAR (http://jaspar.genereg.net/). The different fragment sequences were synthesized and then inserted into a pGL3-basic vector (Promega). All vectors were verified by sequencing, and their luciferase activities were assessed using the Dual Luciferase Assay Kit (Promega), according to the manufacturer's instructions.

ChIP Assays

BGC-823 and AGS cells were treated with formaldehyde and incubated for 10 min to generate DNA-protein cross-links. Cell lysates were then sonicated to generate chromatin fragments of 200–300 bp, and the lysates were immunoprecipitated with EZH2, LSD1, and H3K27me and an H3K4me2-specific antibody (Millipore), or IgG as the control. The precipitated chromatin DNA was recovered and analyzed by qRT-PCR.

Fluorescence In Situ Hybridization and Subcellular Fractionation

BGC823 and AGS cells were fixed in 4% formaldehyde for 15 min and then washed with PBS. The fixed cells were treated with pepsin (1% in 10 mM HCl) and dehydrated through 70%, 90%, and 100% ethanol. The air-dried cells were incubated further with 40 nM of the FISH probe in hybridization buffer (100 mg/mL dextran sulfate, 10% formamide in 2× saline sodium citrate [SSC]) at 80°C for 2 min. Hybridization was performed at 55°C for 2 hr, and the slide was washed and dehydrated. Finally, the air-dried slide was mounted with Prolong Gold Antifade Reagent with 4′,6-diamidino-2-phenylindole (DAPI) for detection. RNA FISH probes were designed and synthesized by Bogu. Nuclear and cytosolic fraction separation was performed using a PARIS kit (Life Technologies), according to the manufacturer's instructions.

Western Blotting and Antibodies

BGC823 and AGS cells were lysed with RIPA extraction reagent (Beyotime) supplemented with a protease inhibitor cocktail (Roche). Proteins (40 μg) were separated by 10% SDS-PAGE, transferred to 0.22 μm polyvinylidene fluoride membranes (Millipore), and then incubated with CADM4, LATS2, KLF2, or glyceraldehyde 3-phosphate dehydrogenase (GAPDH) (Abcam) antibodies. Enhanced

chemiluminescence (ECL) chromogenic substrate was used for protein visualization, and the proteins were quantified by densitometry (Quantity One software; Bio-Rad). All antibodies are listed in Table S1.

Statistical Analysis

The Student's t test (two-tailed), one-way analysis of variance, and the Mann-Whitney U test were conducted to analyze the in vitro and in vivo data by SPSS 17.0 software (IBM). P values less than 0.05 were considered significant.

SUPPLEMENTAL INFORMATION

Supplemental Information includes four figures and three tables can be found with this article online at http://dx.doi.org/10.1016/j.ymthe.2017.01.017.

AUTHOR CONTRIBUTIONS

M.S., F.N., and Z.W. acquired data, drafted of the manuscript, and critically revised the manuscript for important intellectual content; M.H. performed in vitro and in vivo assays; Y.W. and J.H. analyzed and interpreted data and statistical analysis; M.X. and C.W. provided technical or material support; M.S., F.N., and Z.W. approved the final version of the manuscript.

CONFLICTS OF INTEREST

The authors declare no conflicts of interest.

ACKNOWLEDGMENTS

This work was supported by grants from the National Natural Science Foundation of China (nos. 81272601 and 81472198 to Z.W. and 81602013 to F.N.) and the Key Clinical Medicine Technology Foundation of Jiangsu Province (no. BL2014096 to Z.W.). M.S. was supported by the University of Texas MD Anderson Odyssey Program.

REFERENCES

1. Jemal, A., Bray, F., Center, M.M., Ferlay, J., Ward, E., and Forman, D. (2011). Global cancer statistics. CA Cancer J. Clin. *61*, 69–90.
2. Siegel, R., Ma, J., Zou, Z., and Jemal, A. (2014). Cancer statistics, 2014. CA Cancer J. Clin. *64*, 9–29.
3. Siegel, R., Naishadham, D., and Jemal, A. (2013). Cancer statistics, 2013. CA Cancer J. Clin. *63*, 11–30.
4. Chen, W., Zheng, R., Baade, P.D., Zhang, S., Zeng, H., Bray, F., Jemal, A., Yu, X.Q., and He, J. (2016). Cancer statistics in China, 2015. CA Cancer J. Clin. *66*, 115–132.
5. Jang, B.G., and Kim, W.H. (2011). Molecular pathology of gastric carcinoma. Pathobiology *78*, 302–310.
6. Yarmishyn, A.A., and Kurochkin, I.V. (2015). Long noncoding RNAs: a potential novel class of cancer biomarkers. Front. Genet. *6*, 145.
7. Fatima, R., Akhade, V.S., Pal, D., and Rao, S.M. (2015). Long noncoding RNAs in development and cancer: potential biomarkers and therapeutic targets. Mol. Cell. Ther. *3*, 5.
8. Djebali, S., Davis, C.A., Merkel, A., Dobin, A., Lassmann, T., Mortazavi, A., Tanzer, A., Lagarde, J., Lin, W., Schlesinger, F., et al. (2012). Landscape of transcription in human cells. Nature *489*, 101–108.
9. Harrow, J., Frankish, A., Gonzalez, J.M., Tapanari, E., Diekhans, M., Kokocinski, F., Aken, B.L., Barrell, D., Zadissa, A., Searle, S., et al. (2012). GENCODE: the reference human genome annotation for The ENCODE Project. Genome Res. *22*, 1760–1774.
10. Nagano, T., and Fraser, P. (2011). No-nonsense functions for long noncoding RNAs. Cell *145*, 178–181.
11. Wapinski, O., and Chang, H.Y. (2011). Long noncoding RNAs and human disease. Trends Cell Biol. *21*, 354–361.
12. Shi, X., Sun, M., Liu, H., Yao, Y., and Song, Y. (2013). Long non-coding RNAs: a new frontier in the study of human diseases. Cancer Lett. *339*, 159–166.
13. Sahu, A., Singhal, U., and Chinnaiyan, A.M. (2015). Long noncoding RNAs in cancer: from function to translation. Trends Cancer *1*, 93–109.
14. Yan, X., Hu, Z., Feng, Y., Hu, X., Yuan, J., Zhao, S.D., Zhang, Y., Yang, L., Shan, W., He, Q., et al. (2015). Comprehensive genomic characterization of long non-coding RNAs across human cancers. Cancer Cell *28*, 529–540.
15. Liu, X.H., Sun, M., Nie, F.Q., Ge, Y.B., Zhang, E.B., Yin, D.D., Kong, R., Xia, R., Lu, K.H., Li, J.H., et al. (2014). Lnc RNA HOTAIR functions as a competing endogenous RNA to regulate HER2 expression by sponging miR-331-3p in gastric cancer. Mol. Cancer *13*, 92.
16. Liu, Y.W., Sun, M., Xia, R., Zhang, E.B., Liu, X.H., Zhang, Z.H., Xu, T.P., De, W., Liu, B.R., and Wang, Z.X. (2015). LincHOTAIR epigenetically silences miR34a by binding to PRC2 to promote the epithelial-to-mesenchymal transition in human gastric cancer. Cell Death Dis. *6*, e1802.
17. Xie, M., Sun, M., Zhu, Y.N., Xia, R., Liu, Y.W., Ding, J., Ma, H.W., He, X.Z., Zhang, Z.H., Liu, Z.J., et al. (2015). Long noncoding RNA HOXA-AS2 promotes gastric cancer proliferation by epigenetically silencing P21/PLK3/DDIT3 expression. Oncotarget *6*, 33587–33601.
18. Nie, F., Yu, X., Huang, M., Wang, Y., Xie, M., Ma, H., Wang, Z., De, W., and Sun, M. (2016). Long noncoding RNA ZFAS1 promotes gastric cancer cells proliferation by epigenetically repressing KLF2 and NKD2 expression. Oncotarget.
19. Sun, M., Xia, R., Jin, F., Xu, T., Liu, Z., De, W., and Liu, X. (2014). Downregulated long noncoding RNA MEG3 is associated with poor prognosis and promotes cell proliferation in gastric cancer. Tumour Biol. *35*, 1065–1073.
20. Sun, M., Jin, F.Y., Xia, R., Kong, R., Li, J.H., Xu, T.P., Liu, Y.W., Zhang, E.B., Liu, X.H., and De, W. (2014). Decreased expression of long noncoding RNA GAS5 indicates a poor prognosis and promotes cell proliferation in gastric cancer. BMC Cancer *14*, 319.
21. Childs, E.J., Mocci, E., Campa, D., Bracci, P.M., Gallinger, S., Goggins, M., Li, D., Neale, R.E., Olson, S.H., Scelo, G., et al. (2015). Common variation at 2p13.3, 3q29, 7p13 and 17q25.1 associated with susceptibility to pancreatic cancer. Nat. Genet. *47*, 911–916.
22. Zheng, J., Huang, X., Tan, W., Yu, D., Du, Z., Chang, J., Wei, L., Han, Y., Wang, C., Che, X., et al. (2016). Pancreatic cancer risk variant in LINC00673 creates a miR-1231 binding site and interferes with PTPN11 degradation. Nat. Genet. *48*, 747–757.
23. Shi, X., Ma, C., Zhu, Q., Yuan, D., Sun, M., Gu, X., Wu, G., Lv, T., and Song, Y. (2016). Upregulation of long intergenic noncoding RNA 00673 promotes tumor proliferation via LSD1 interaction and repression of NCALD in non-small-cell lung cancer. Oncotarget *7*, 25558–25575.
24. Li, H., Yu, B., Li, J., Su, L., Yan, M., Zhang, J., Li, C., Zhu, Z., and Liu, B. (2015). Characterization of differentially expressed genes involved in pathways associated with gastric cancer. PLoS ONE *10*, e0125013.
25. Wu, Y., Grabsch, H., Ivanova, T., Tan, I.B., Murray, J., Ooi, C.H., Wright, A.I., West, N.P., Hutchins, G.G., Wu, J., et al. (2013). Comprehensive genomic meta-analysis identifies intra-tumoural stroma as a predictor of survival in patients with gastric cancer. Gut *62*, 1100–1111.
26. Sun, M., Liu, X.H., Lu, K.H., Nie, F.Q., Xia, R., Kong, R., Yang, J.S., Xu, T.P., Liu, Y.W., Zou, Y.F., et al. (2014). EZH2-mediated epigenetic suppression of long noncoding RNA SPRY4-IT1 promotes NSCLC cell proliferation and metastasis by affecting the epithelial-mesenchymal transition. Cell Death Dis. *5*, e1298.
27. Lu, K.H., Li, W., Liu, X.H., Sun, M., Zhang, M.L., Wu, W.Q., Xie, W.P., and Hou, Y.Y. (2013). Long non-coding RNA MEG3 inhibits NSCLC cells proliferation and induces apoptosis by affecting p53 expression. BMC Cancer *13*, 461.
28. Zhang, E.B., Kong, R., Yin, D.D., You, L.H., Sun, M., Han, L., Xu, T.P., Xia, R., Yang, J.S., De, W., and Chen, Jf. (2014). Long noncoding RNA ANRIL indicates a poor

prognosis of gastric cancer and promotes tumor growth by epigenetically silencing of miR-99a/miR-449a. Oncotarget *5*, 2276–2292.

29. Kaczynski, J., Cook, T., and Urrutia, R. (2003). Sp1- and Krüppel-like transcription factors. Genome Biol. *4*, 206.

30. Pearson, R., Fleetwood, J., Eaton, S., Crossley, M., and Bao, S. (2008). Krüppel-like transcription factors: a functional family. Int. J. Biochem. Cell Biol. *40*, 1996–2001.

31. Bureau, C., Hanoun, N., Torrisani, J., Vinel, J.P., Buscail, L., and Cordelier, P. (2009). Expression and function of Kruppel like-factors (KLF) in carcinogenesis. Curr. Genomics *10*, 353–360.

32. Zhang, W., Levi, L., Banerjee, P., Jain, M., and Noy, N. (2015). Kruppel-like factor 2 suppresses mammary carcinoma growth by regulating retinoic acid signaling. Oncotarget *6*, 35830–35842.

33. Visser, S., and Yang, X. (2010). LATS tumor suppressor: a new governor of cellular homeostasis. Cell Cycle *9*, 3892–3903.

34. Takahashi, Y., Miyoshi, Y., Takahata, C., Irahara, N., Taguchi, T., Tamaki, Y., and Noguchi, S. (2005). Down-regulation of LATS1 and LATS2 mRNA expression by promoter hypermethylation and its association with biologically aggressive phenotype in human breast cancers. Clin. Cancer Res. *11*, 1380–1385.

35. Murakami, H., Mizuno, T., Taniguchi, T., Fujii, M., Ishiguro, F., Fukui, T., Akatsuka, S., Horio, Y., Hida, T., Kondo, Y., et al. (2011). LATS2 is a tumor suppressor gene of malignant mesothelioma. Cancer Res. *71*, 873–883.

36. Furth, N., Bossel Ben-Moshe, N., Pozniak, Y., Porat, Z., Geiger, T., Domany, E., Aylon, Y., and Oren, M. (2015). Down-regulation of LATS kinases alters p53 to promote cell migration. Genes Dev. *29*, 2325–2330.

YMTHE, Volume *25*

Supplemental Information

Long Noncoding RNA LINC00673 Is Activated by SP1 and Exerts Oncogenic Properties by Interacting with LSD1 and EZH2 in Gastric Cancer

Mingde Huang, Jiakai Hou, Yunfei Wang, Min Xie, Chenchen Wei, Fengqi Nie, Zhaoxia Wang, and Ming Sun

Supplementary Table1. Primers, siRNAs and shRNAs sequence

Primers for qPCR	
GAPDH F	GGGAGCCAAAAGGGTCAT
GAPDH R	GAGTCCTTCCACGATACCAA
LINC00673 F	TACCACACCCTTTCTTGCCC
LINC00673 R	ACACTGGCCTCTTTACACGG
LINC00673 P1 F	CATAGCCTGGGACTTGAA
LINC00673 P1 R	CATGAGAATCGCTTGGAC
LINC00673 P2 F	GGAATGCCCTGTCTATCT
LINC00673 P2 R	GGCATGAGAATCGCTTGG
CADM4 F	CTAGTGGGCATGGTCTGGTG
CADM4 R	TCCCTGTTCATCCAAGCCAC
CLDN6 F	CATGCCATCATCCGGGACTT
CLDN6 R	GCAGGGGCAGATGTTGAGTA
EMP3 F	TCTACACCATGCGACGAGGA
EMP3 R	GGGCGAAGCAGTATCCGAAG
GADD45GIP1 F	GTGGTCCCCGGTTCGTTATG
GADD45GIP1 R	CAGTATCCAGTCCCGCCATC
INHBE F	TCTTGGACACAGCAGGACAC
INHBE R	CAGTATCCAGTCCCGCCATC
KIF14 F	CGGGATTGACGGCAGTAAGA
KIF14 R	ACTGGGTGTGCATTCCTCTG
S100P F	AGTTCATCGTGTTCGTGGCT
S100P R	CACTTTTGGGAAGCCTGGGA
E2F2 F	CCAGCGCATCGCGTCTC
E2F2 R	TAGAGATCGCCGCTTGGAG
CRIP2 F	GTGCGACAAGACCGTGTACT
CRIP2 R	TCGCACTTGAGGCAGAACTT
KLF2 P26-155 F	ACGGGCTTATTGAGGTTGG
KLF2 P26-155 R	GCCTGGGTGACAGAGGAGAC
KLF2 F	AGAGGGTCTCCCTCGATGAC
KLF2 R	TCTCACAAGGCATCACAAGC
LATS2 F	ACCCCAAAGTTCGGACCTTAT
LATS2 R	CATTTGCCGGTTCACTTCTGC
siRNA sequence	
si-LINC00673 1#	CAGCCGGAUACAGAGUGAAUAGUUA
si-LINC00673 2#	UGUGCCUUUGUACUCAGCAAUUCUU
si-SP1-1	CAGCGUUUCUGCAGCUACCUUGACU
si-SP1-2	GACAGGUCAGUUGGCAGACUCUACA

si-EZH2-1	AAGACTCTGAATGCAGTTGCT
si-EZH2-2	CGGCUUCCCAAUAACAGUATT
si-LSD1-1	CAACCTCTCAGAAGATGAGTATTAT
si-LSD1-2	CAAAGGAAACTATGTAGCTGATCTT
si-KLF2	CCAAGAGTTCGCATCTGAA
si-LATS2	CAGGTGGACTCACAATTCCAAATAT
shRNA sequence	
sh-LINC00673 1#	CACCGCAGCCGGATACAGAGTGAATAGTTACGAATAACTAT TCACTCTGTATCCGGCTG
sh-LINC00673 2#	CACCGTGTGCCTTTGTACTCAGCAATTCTTCGAAAAGAATTG CTGAGTACAAAGGCACA

Supplementary Table 2. Correlation between LINC00673 expression and clinicopathological characteristics of gastric cancer patients (n = 73)

Characteristics	**Linc00673 Low no. case(%)**	**Linc00673 High no. case(%)**	**P Chi-squared test P-value**
Age(years)			
>65	18(24.7)	16(21.9)	0.352
≤65	25(34.2)	14(19.2)	
Gender			
Male	23(31.5)	19(26.0)	0.474
Female	20(27.4)	11(15.1)	
Histologic			
Well	20(27.4)	4(5.8)	
Moderately	15(20.5)	15(20.5)	0.026*
Poorly	7(9.6)	9(12.3)	
Undifferentiated	1(1.4)	2(2.7)	
TNM Stage			
I	7(9.6)	0(0.0)	
II	18(24.7)	10(13.7)	0.024*
III	16(21.9)	14(19.2)	
IV	2(2.7)	6(8.2)	
Tumor size			
≤5cm	28(38.4)	11(15.1)	0.019*
>5cm	15(20.5)	19(26.0)	
Lymph node metastasis			
Negative	19(26.0)	6(8.2）	0.045*
Positive	24(32.9)	24(32.9)	
Location			
Distal	17(23.3)	14(19.2)	0.741
Middle	15(20.5)	8(11.0)	
Proximal	11(15.1)	8(11.0)	

Supplementary Table 3. Univariate and multivariate analysis of OS in gastric cancer patients (n=73)

Variables	Univariate analysis			Multivariate analysis		
	HR	95% CI	p value	HR	95% CI	p value
Age	0.855	0.435-1.683	0.651			
Gender	0.836	0.436-1.605	0.591			
Location	1.232	0.779-1.950	0.372			
Tumor size	1.618	0.846-3.095	0.146			
Histologic	1.742	1.165-2.606	0.007*	1.395	0.903-2.156	0.134
TNM stage	1.695	1.087-2.643	0.020*	1.217	0.725-2.043	0.458
Lymph node metastasis (No vs .Yes)	3.766	1.539-9.217	0.004*	2.556	1.014-6.444	0.047*
LINC00673 expression (High vs. Low)	4.010	2.017-7.969	<0.001*	2.381	1.121-5.056	0.024*

HR, hazard ratio; 95 % CI, 95 % confidence interval, * Overall P < 0.05.

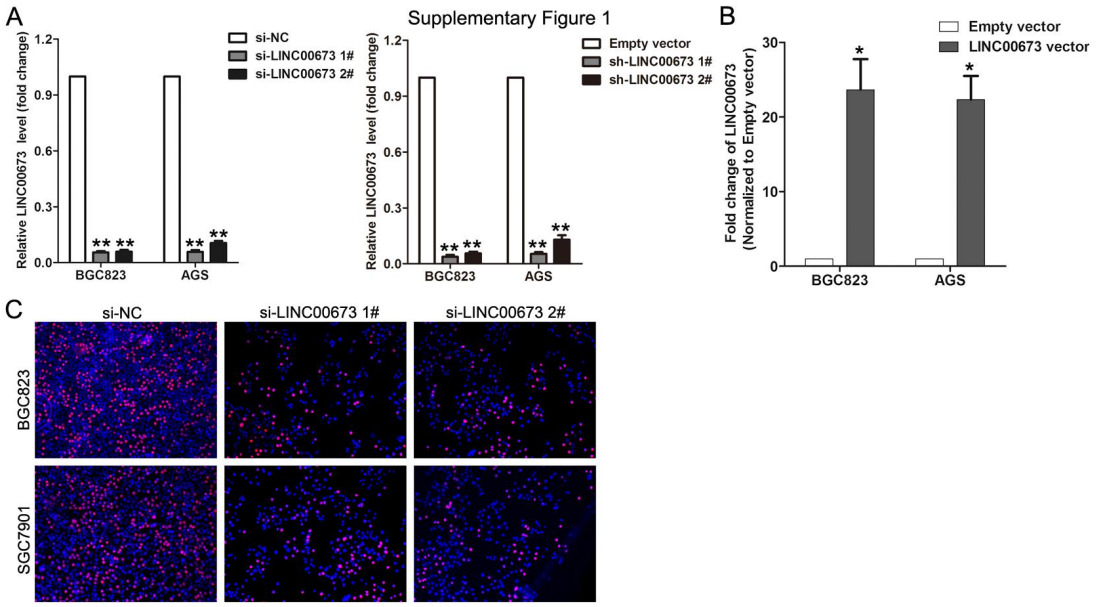

Figure S1. (a) qRT-PCR analysis of LINC00673 expression in BGC823 and AGS cells after transfection with si-DUXAP8 or sh-DUXAP8. **(b)** qRT-PCR analysis of LINC00673 expression in BGC823 and AGS cells after transfection with the LINC00673 expression vector or an empty vector. **(c)** Cell proliferation of BGC823 and AGS was evaluated 48 h after transfection with LINC00673 or NC siRNA using EdU-incorporation assays. Red: EdU staining of proliferating cells; blue: DAPI staining of the cell nuclei. The mean values and standard errors were calculated from triplicates of a representative experiment. *P<0.05, **P<0.01.

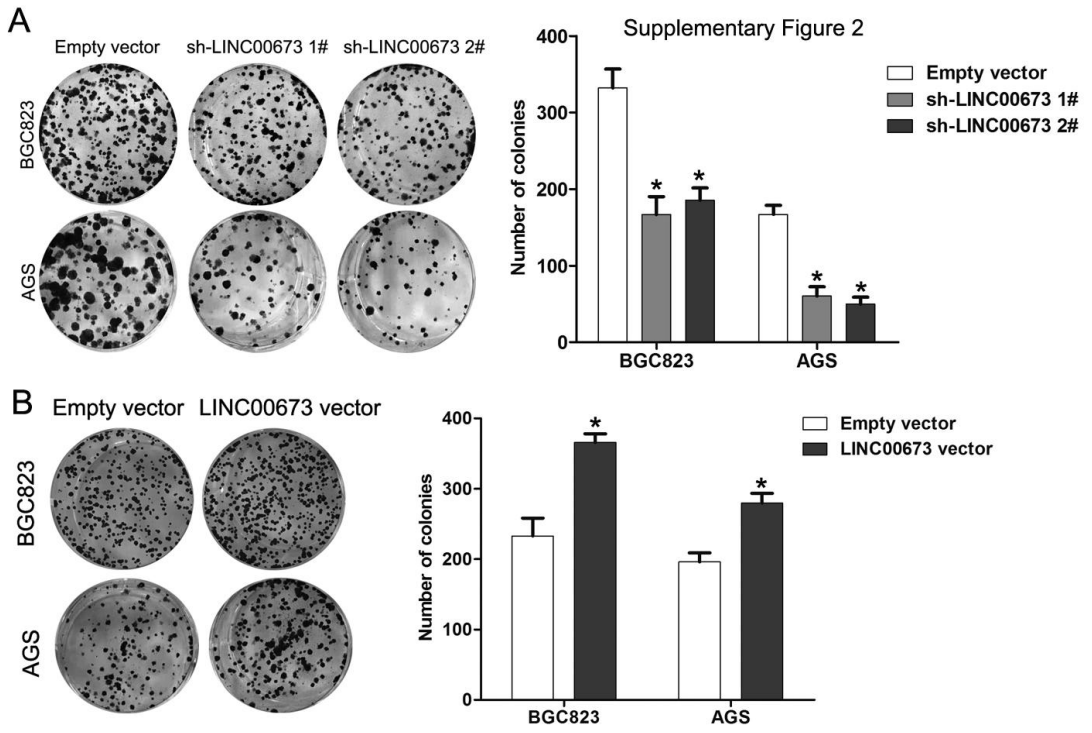

Figure S2. (a) Colony formation analysis of BGC823 and AGS cell proliferation after transfection with sh-LIN00673 or an empty vector. **(b)** Colony formation analysis of BGC823 and AGS cell proliferation after transfection with the LINC0673 expression vector or an empty vector. The mean values and standard errors were calculated from triplicates of a representative experiment. *P<0.05.

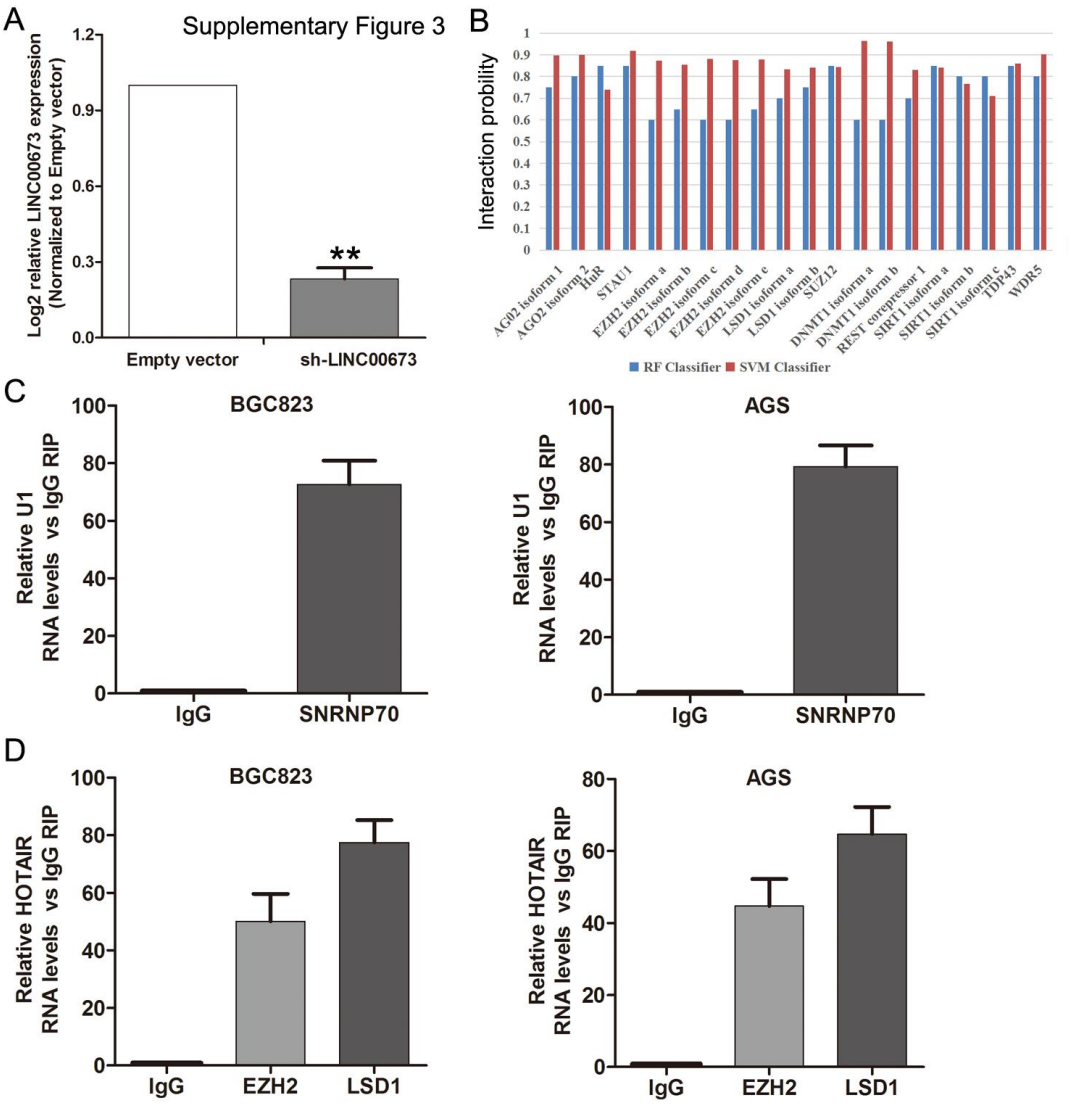

Supplementary Figure 3. (a) qRT-PCR analysis of LINC00673 expression in mouse tumor tissues from sh-LINC00673 or the control group. **(b)** Prediction of the interaction probability between LINC00673 and RNA binding proteins using the online database at http://pridb.gdcb.iastate.edu/RPISeq/. **(c)** U1 RNA levels in SNRNP70 immunoprecipitates were determined by qRT-PCR. The expression levels for U1 RNA are presented as fold enrichment values relative to the IgG immunoprecipitates. **(d)** HOTAIR RNA levels in EZH2 and LSD1 immunoprecipitates were determined by qRT-PCR. Expression levels for HOTAIR are presented as fold enrichment values relative to the IgG immunoprecipitates. The mean values and standard errors were calculated from triplicates of a representative experiment. **P<0.01.

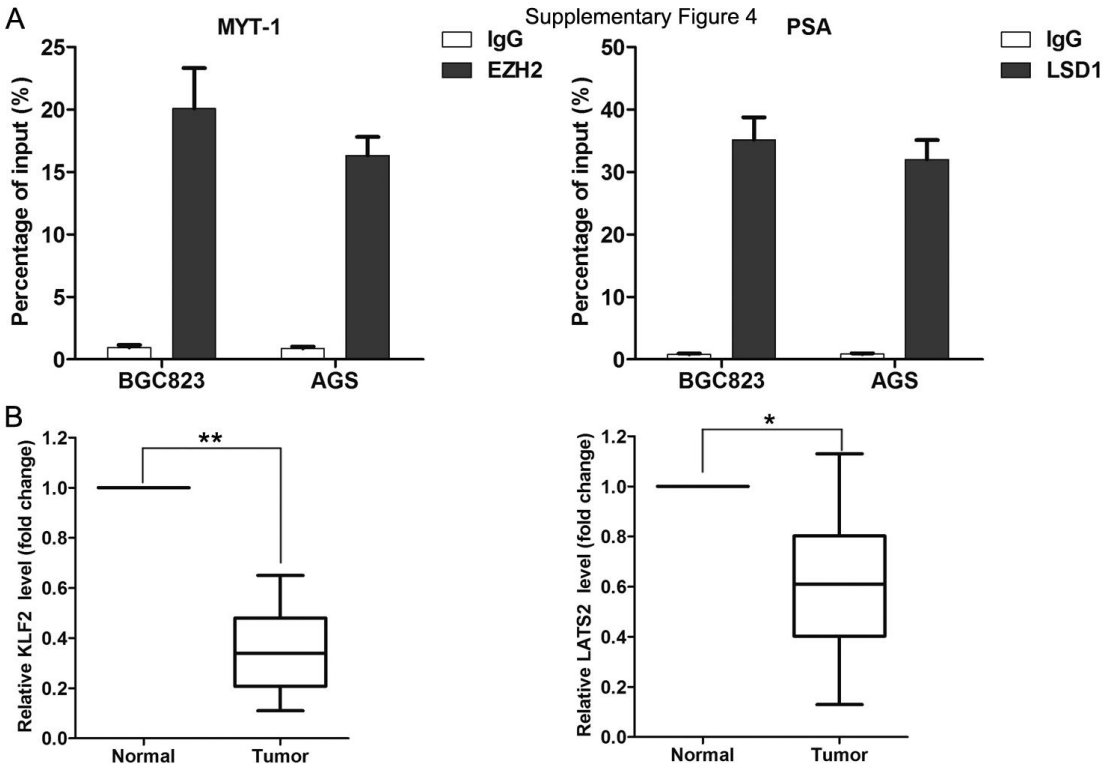

Supplementary Figure 4. (a) ChIP-qPCR analysis of EZH2 or LSD1 occupancy in the MYT-1 and PSA promoters in BGC823 and AGS cells, with IgG used as the negative control. **(b)** qRT-PCR analysis of KLF2 and LATS2 expression in 20 paired GC tumor tissues and their adjacent non-tumor tissues. The mean values and standard errors were calculated from triplicates of a representative experiment. *P<0.05, **P<0.01.